

Thoracic aortic disease in tuberous sclerosis complex: molecular pathogenesis and potential therapies in *Tsc2*^{+/-} mice

Jiumei Cao^{1,4}, Limin Gong¹, Dong-chuan Guo¹, Ulrike Mietzsch², Shao-Qing Kuang¹, Callie S. Kwartler¹, Hazim Safi³, Anthony Estrera³, Michael J. Gambello² and Dianna M. Milewicz^{1,*}

¹Department of Internal Medicine, ²Department of Pediatrics and ³Department of Cardiothoracic and Vascular Surgery, University of Texas Medical School at Houston, Houston, TX 77030, USA and ⁴Department of Cardiology, Rui Jin Hospital, Jiaotong University School of Medicine, Shanghai 200025, PR China

Received October 28, 2009; Revised and Accepted February 12, 2010

Tuberous sclerosis complex (TSC) is a genetic disorder with pleiotropic manifestations caused by heterozygous mutations in either *TSC1* or *TSC2*. One of the less investigated complications of TSC is the formation of aneurysms of the descending aorta, which are characterized on pathologic examination by smooth muscle cell (SMC) proliferation in the aortic media. SMCs were explanted from *Tsc2*^{+/-} mice to investigate the pathogenesis of aortic aneurysms caused by *TSC2* mutations. *Tsc2*^{+/-} SMCs demonstrated increased phosphorylation of mammalian target of rapamycin (mTOR), S6 and p70S6K and increased proliferation rates compared with wild-type (WT) SMCs. *Tsc2*^{+/-} SMCs also had reduced expression of SMC contractile proteins compared with WT SMCs. An inhibitor of mTOR signaling, rapamycin, decreased SMC proliferation and increased contractile protein expression in the *Tsc2*^{+/-} SMCs to levels similar to WT SMCs. Exposure to α -elastin fragments also decreased proliferation of *Tsc2*^{+/-} SMCs and increased levels of p27^{kip1}, but failed to increase expression of contractile proteins. In response to artery injury using a carotid artery ligation model, *Tsc2*^{+/-} mice significantly increased neointima formation compared with the control mice, and the neointima formation was inhibited by treatment with rapamycin. These results demonstrate that *Tsc2* haploinsufficiency in SMCs increases proliferation and decreases contractile protein expression and suggest that the increased proliferative potential of the mutant cells may be suppressed *in vivo* by interaction with elastin. These findings provide insights into the molecular pathogenesis of aortic disease in TSC patients and identify a potential therapeutic target for treatment of this complication of the disease.

INTRODUCTION

Tuberous sclerosis complex (TSC) is an autosomal dominant disorder with pleiotropic manifestations due to mutations in either *TSC1* (hamartin) or *TSC2* (tuberin) (1–3). The disorder affects the brain (cortical and subcortical tubers, subependymal nodules and giant cell astrocytomas), kidneys (angiomyolipomas, cysts, carcinoma), skin (hypomelanotic macules, shagreen patches, facial angiofibromas, periungual fibromas), eyes (retinal hamartomas), heart (rhabdomyomas) and other organs. *TSC1* and *TSC2* are ubiquitously expressed and

form heterodimers that inhibit the activation of mammalian target of rapamycin (mTOR) signaling (4–6). The *TSC1/TSC2* complex negatively regulates mTOR through GTPase-activating protein (GAP) activity directed at the small GTPase Rheb (Ras homolog enriched in brain), which binds and activates mTOR. When associated with the proteins raptor and mLST8, mTOR exists in a rapamycin-sensitive complex, termed mTORC1. Loss of either *TSC1* or *TSC2* abolishes the Rheb-GTPase activity, resulting in constitutively activated mTORC1. The activated mTORC1 kinase then enhances protein translation by phosphorylation of S6K1 and

*To whom correspondence should be addressed. Tel: +1 7135006715; Fax: +1 7135000693; Email: dianna.m.milewicz@uth.tmc.edu

eukaryotic translation-initiation factor 4E-binding protein 1 (4E-BP1) (7–9). S6K1 is a kinase that activates ribosomal subunit protein S6, leading to ribosome recruitment and protein translation. 4E-BP1 inhibits the activity of eukaryotic translation-initiation factor 4E (eIF4E), and when phosphorylated by mTORC1, releases eIF4E from its control (10). Therefore, mTORC1 activation promotes cell growth, cell cycle progression and proliferation, in part by increasing the anabolic process of protein synthesis through the activation of S6K and the inhibition of 4E-BP1 (11,12).

An unusual and less recognized complication of TSC is vascular abnormalities, which include very premature onset of aortic aneurysms in infants, children and young adults. Aortic aneurysms are extremely rare in infants, and the youngest reported TSC case is an infant who died of aortic aneurysm rupture at the age of 4.5 months (13). TSC patients primarily have abdominal aortic aneurysms and the majority of these aneurysms occur in children below the age of 5 years. The pathogenesis of aortic aneurysms in these TSC patients remains largely unknown despite the fact that these aneurysms can lead to premature death in TSC (13–17). Surprisingly, none of the case reports in the literature indicates whether the aortic aneurysms were associated with *TSC1* or *TSC2* mutations.

Vascular smooth muscle cells (SMCs) are not terminally differentiated and maintain a phenotypic plasticity that allows for transition from quiescent, differentiated cells expressing a repertoire of proteins required for contractile function (α -actin, calponin and β -myosin heavy chain) to proliferating, migrating cells with loss of contractile protein expression and increased synthesis of extracellular matrix proteins. SMCs are differentiated cells in a mature, functional artery but de-differentiate with vascular injury and environmental cues. In SMCs, mTORC1 signaling is already known to influence SMC differentiation; inhibition of mTORC1 signaling with the macrolide antibiotic rapamycin promotes SMC differentiation through the activation of the Akt pathway and the induction of contractile protein expression (18,19).

We confirmed a *TSC2* mutation in a 3-year-old male with a large thoracoabdominal aneurysm. On the basis of this knowledge, we investigated the role of *TSC2* deficiency on aortic SMC differentiation and proliferation using a heterozygous *Tsc2*-deficient mouse model. We found that the activation of the mTORC1 pathway with *Tsc2* deficiency leads to SMC proliferation and de-differentiation *in vitro* and *in vivo*, which can be reversed with rapamycin treatment. Interestingly, exposure to α -elastin peptides also reduced *Tsc2*^{+/-} SMC proliferation but did not increase the expression of contractile proteins in the mutant SMCs *in vitro*.

RESULTS

Descending aortic aneurysm associated with subintimal SMC proliferation in a child with a *TSC2* mutation

An African-American boy was diagnosed with TSC at 5 months of age when he presented with generalized tonic-clonic seizures and multiple hypopigmented macules. Computerized tomography of the brain at that time showed multiple subependymal nodules, and tubers in the left parietal and frontal lobes. Genetic testing identified a 32 bp deletion from the nucleotide

position of 5340–5371 in *TSC2*, codon position 1780–1791, which causes a frame shift mutation and truncation of the protein. Analysis of the parents' DNA determined that the mutation was *de novo*. At the age of 3 years, a magnetic resonance angiogram (MRA) revealed a complex thoracoabdominal aneurysm with three discrete fusiform dilations, with the widest transverse diameter measuring 7 cm and spanning a length of 12 cm (Fig. 1A). The patient underwent surgical repair of the aneurysm, and the pathology of the aorta was examined. The control aorta demonstrated typical organization of the aortic media composed of layers of elastic fibers, with SMCs between these layers. The patient's aorta showed areas of relatively normal aortic media, along with regions of excessive extracellular matrix deposition and nodules of SMCs, confirmed by SMC α -actin staining (Fig. 1C, arrows). Movat pentachrome staining of the aorta confirmed that the SMC proliferation was associated with collagen deposition and occurred in the subintimal layer of the aortic media (Fig. 1C, blue arrowheads indicate the internal elastic lamina—IEL).

Ten months after the initial repair, the patient was clinically asymptomatic on a β -adrenergic blocker but a CT angiography showed new aortic enlargement in the thoracic part of the aorta, the largest transverse diameter measuring 6.5 cm (Fig. 1B). He underwent a second surgical repair. The histology was identical with the previous specimen, except for increased loss of SMCs in the muscular media. He tolerated surgical repair, and 12 months after the second repair, no recurrence of the aneurysm was evident.

Increased proliferation and decreased contractile protein expression in *Tsc2*^{+/-} SMCs

The unique presentation of an aneurysm in a child with a *TSC2* mutation and the associated aortic subintimal SMCs proliferation led us to study the effect of *Tsc2* mutations on vascular SMCs using a mouse model with the deletion of one allele of the *Tsc2* gene (20,21). On the basis of aortic disease presenting in the descending aorta in TSC patients, we hypothesized that loss of *TSC2* would have a differential effect on SMCs of mesodermal origin (descending aorta) versus SMCs that were neural crest-derived (ascending aorta) (22). Therefore, we explanted SMCs of wild-type (WT) and *Tsc2*^{+/-} mice from the ascending and descending aorta separately, seeded the cells at the same density with serum deprivation and assessed proliferation by bromodeoxyuridine (BrdU) incorporation in SMCs. In WT SMCs, proliferation rates did not differ between ascending and descending aortic SMCs (Fig. 2A). The *Tsc2*^{+/-} SMCs from both the ascending and descending aorta proliferated significantly more rapidly than the WT SMCs, with mutant SMCs from descending aorta proliferated significantly faster than cells explanted from the ascending aorta. Since the descending aorta is primarily involved in TSC patients, further experiments were focused primarily on the descending aortic *Tsc2*^{+/-} SMCs. To examine the cell cycle progression of descending aortic SMCs, cell cycle distribution was analyzed by flow cytometric cell-sorting technique (Fig. 2B). Cell numbers at S and G2/M phases were increased in SMCs explanted from the *Tsc2*^{+/-} SMCs compared with the WT SMCs, indicating that more *Tsc2*^{+/-} cells have entered the cell cycle for proliferation. *TSC1/TSC2* acts to

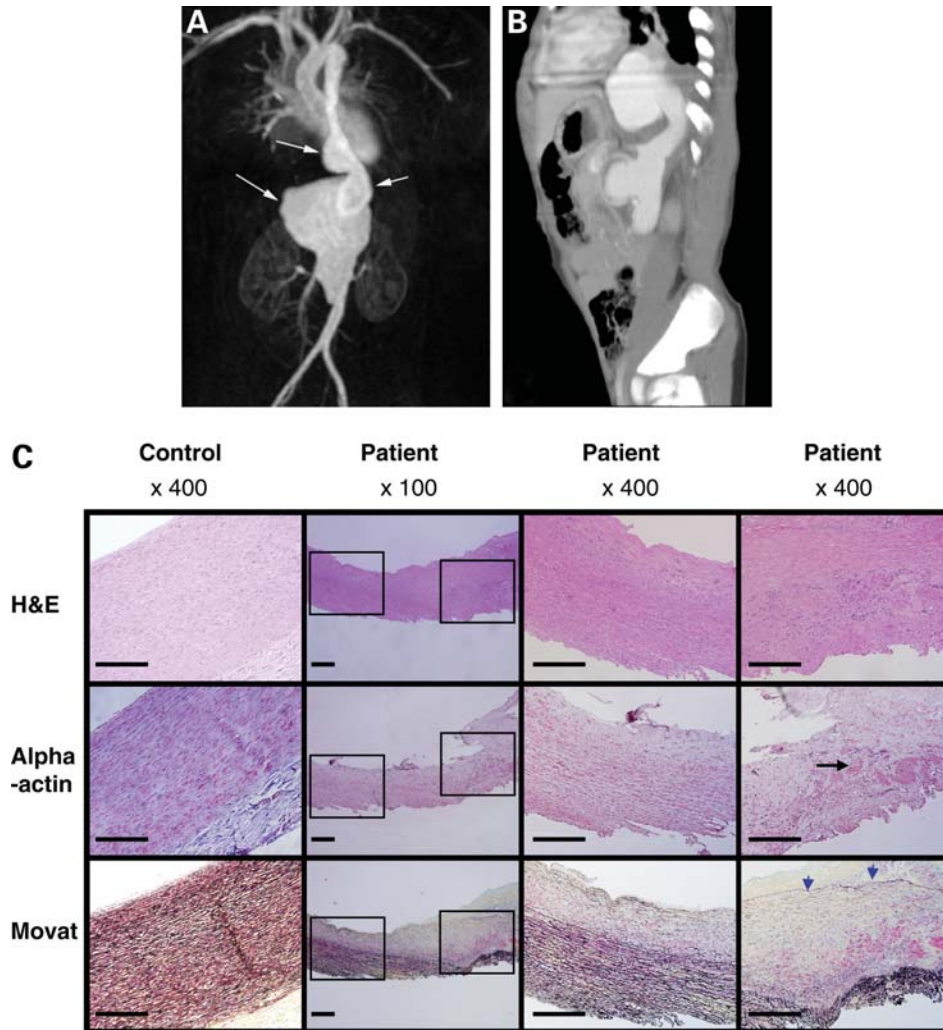


Figure 1. MRA and pathological examination of the aorta of a patient with *TSC2* mutation. (A) A coronal maximum intensity pixel reconstruction from contrast-enhanced MRA demonstrates a multilobulated aneurysm (arrows) involving the distal thoracic and abdominal aorta, with extension below the renal arteries. The distal thoracic aorta harbored the most proximal aneurysm dilation, measuring 2.8 cm in length and 2.4 cm at its greatest diameter. The second fusiform dilation was located in the proximal abdominal aorta, which was 5.3 cm in length, and from which the celiac artery arose. The third fusiform dilation involved the origins of the superior mesenteric artery and both renal arteries. The distal abdominal aorta was normal in caliber, with no involvement of the common iliac arteries. (B) A chest CT with contrast shows two aneurysms in the general region of the proximal and distal graft anastomosis. The first aneurysm is located in the descending thoracic aorta extending anteriorly from the aorta/graft at the level of T8 to L1 and measuring about 6.5 cm in transverse and 3.5 cm in AP dimension. There is a thrombotic layer around the aneurysm that measures about 1.2 cm in thickness. The second aneurysm originates at the level of L1–L2 and extends anteriorly from the abdominal aorta, measuring 3.2 cm in AP dimension \times 3 cm transversely, and involves the origin of the right renal artery. (C) H&E, SMC α -actin and Movat pentachrome staining of aortas from control and TSC patient. H&E staining demonstrates SMC disarray and hyperplasia in the subintimal layer of the media in patient with *TSC2* mutation. α -Actin staining confirms the nodules of cells in the subintimal layer are SMCs in patient's aorta. SMCs in the affected areas of the aorta and from control aorta were quantified by images collection from five fields of vision at \times 400 magnification. Counting of the SMCs confirmed a significant increase of SMCs in patient's affected aorta ($P < 0.005$). Movat staining shows medial disruption in the aorta of the TSC patient that is characterized by nodules of SMCs (red), accumulation of collagen (yellow) and loss and fragmentation of elastic fibers (black). Arrowheads indicate the location of the IEL (stained black), confirming that the pathology occurs primarily in the subintimal layer. Magnification is indicated on each set of panels.

suppress mTORC1 activity, therefore suppressing downstream phosphorylation of S6K and 4E-BP1 (23,24). Immunoblot analysis confirmed increased phosphorylation of Thr389 of S6K in the *Tsc2*^{+/-} descending aortic SMCs compared with WT cells (Fig. 2C). Activation of S6K was also reflected in the increased phosphorylation of its substrate, S6, at both Ser240 and Ser244.

We also sought to determine whether *Tsc2*^{+/-} SMCs were de-differentiated through the assessment of expression of

several contractile proteins, including α -actin (*Acta2*), calponin (*Cnn1*), β -myosin (*Myh11*) and muscular γ -actin (*Actg2*), by quantitative real-time PCR (qPCR) in *Tsc2*^{+/-} SMCs (Fig. 2D). By qPCR, expression of all these contractile proteins were decreased in the mutant SMCs, with the differences more marked in SMCs explanted from the descending aorta compared with ascending aorta. In contrast, expression of the cytoskeleton proteins β -actin (*Actb*) and γ -actin (*Actg1*) were similar between the WT and mutant SMCs

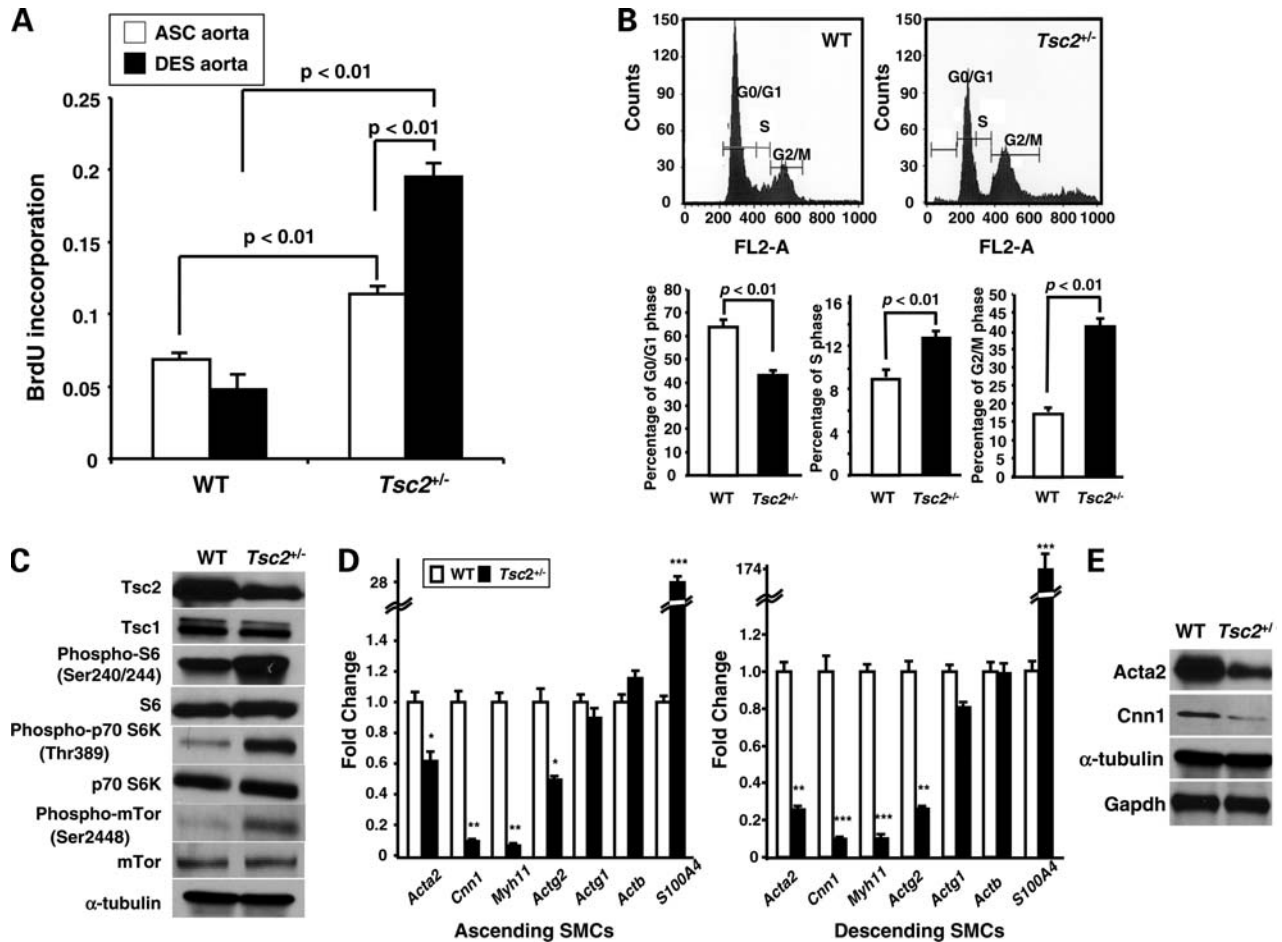


Figure 2. *Tsc2*^{+/-} SMCs demonstrate increased proliferation and decreased expression of contractile proteins. (A) BrdU assay demonstrates that cell proliferation in *Tsc2*^{+/-} mouse SMCs was increased compared with WT SMCs. Proliferation of *Tsc2*^{+/-} SMCs explanted from descending aorta is significantly higher than SMCs explanted from the ascending aorta. (B) Effects of *Tsc2*^{+/-} on cell cycle distribution. After staining with PI, cell cycle distribution was analyzed using a flow cytometer. The data indicated that the number of *Tsc2*^{+/-} SMCs were significantly decreased in G0/G1 phase and significantly increased in S and G2/M phases compared with WT SMCs. Data are reported as means \pm SD of three independent experiments. (C) Increase of the phosphorylation of proteins involved in mTOR signaling pathway in cell lysates from the *Tsc2*^{+/-} SMCs compared with WT SMCs. (D) qPCR analysis of mRNA isolated from SMCs from WT and *Tsc2*^{+/-} aorta. The SMCs explanted from ascending and descending aorta demonstrate that *Tsc2*^{+/-} SMCs have significantly reduced expression of SMC contractile genes, including *Acta2*, *Cnn1* and *Actg2*. In contrast, SMCs from both *Tsc2*^{+/-} and WT mice express similar amounts of cytoskeletal genes, including *Actg1* and *Actb*. *Tsc2*^{+/-} SMCs significantly increase expression of SMC de-differentiation marker, *S100A4*, particularly SMCs explanted from the descending aorta. Gene expression levels are standardized to *Gapdh*. * $P < 0.05$, ** $P < 0.01$, *** $P < 0.001$. (E) Immunoblot analysis of SMC lysates confirms reduced levels of SMC contractile protein in SMCs explanted from *Tsc2*^{+/-} aorta compared with those from WT mice. Protein levels are normalized to *Gapdh*.

(Fig. 2D). Immunoblot analysis of *Tsc2*^{+/-} descending SMCs compared with WT confirmed decreased protein levels of SMC α -actin and calponin (Fig. 2E). Interestingly, expression of *S100A4* was greatly increased in the *Tsc2*^{+/-} SMCs, with a more dramatic increase noted in the descending mutant SMCs. *S100A4* has been shown to be increased in de-differentiated SMCs with enhanced proliferation when compared with differentiated, nonproliferating SMCs (25).

Inhibition of mTORC1 signaling decreases proliferation and increases contractile protein expression in *Tsc2*^{+/-} SMCs

In order to determine whether the increased proliferation and de-differentiation of *Tsc2*^{+/-} SMCs were due to augmented mTORC1 activity, rapamycin was used to inhibit mTORC1 activity. Rapamycin inhibits mTORC1 through the

association with its intracellular receptor, FKBP12, and the FKBP12-rapamycin complex binds directly to the FKBP12-rapamycin-binding (FRB) domain of mTOR (26). After 24 h of rapamycin treatment, phosphorylation of S6K and S6 was decreased in the *Tsc2*^{+/-} and WT cells and remained suppressed for 72 h of rapamycin treatment (Fig. 3A). Rapamycin treatment decreased the proliferation of both the WT and *Tsc2*^{+/-} aortic SMCs, suppressing the proliferation of mutant SMCs to the WT level after 72 h of treatment (Fig. 3B). Furthermore, the number of WT and mutant cells in S and G2/M phases was significantly decreased after treatment with rapamycin (Fig. 3C). These results indicated that rapamycin inhibited SMC proliferation by causing cell cycle arrest at G0/G1 phase, therefore blocking the G1/S transition during cell division in *Tsc2*^{+/-} SMCs.

We also determined whether the decreased proliferation of *Tsc2*^{+/-} SMCs with rapamycin treatment was associated

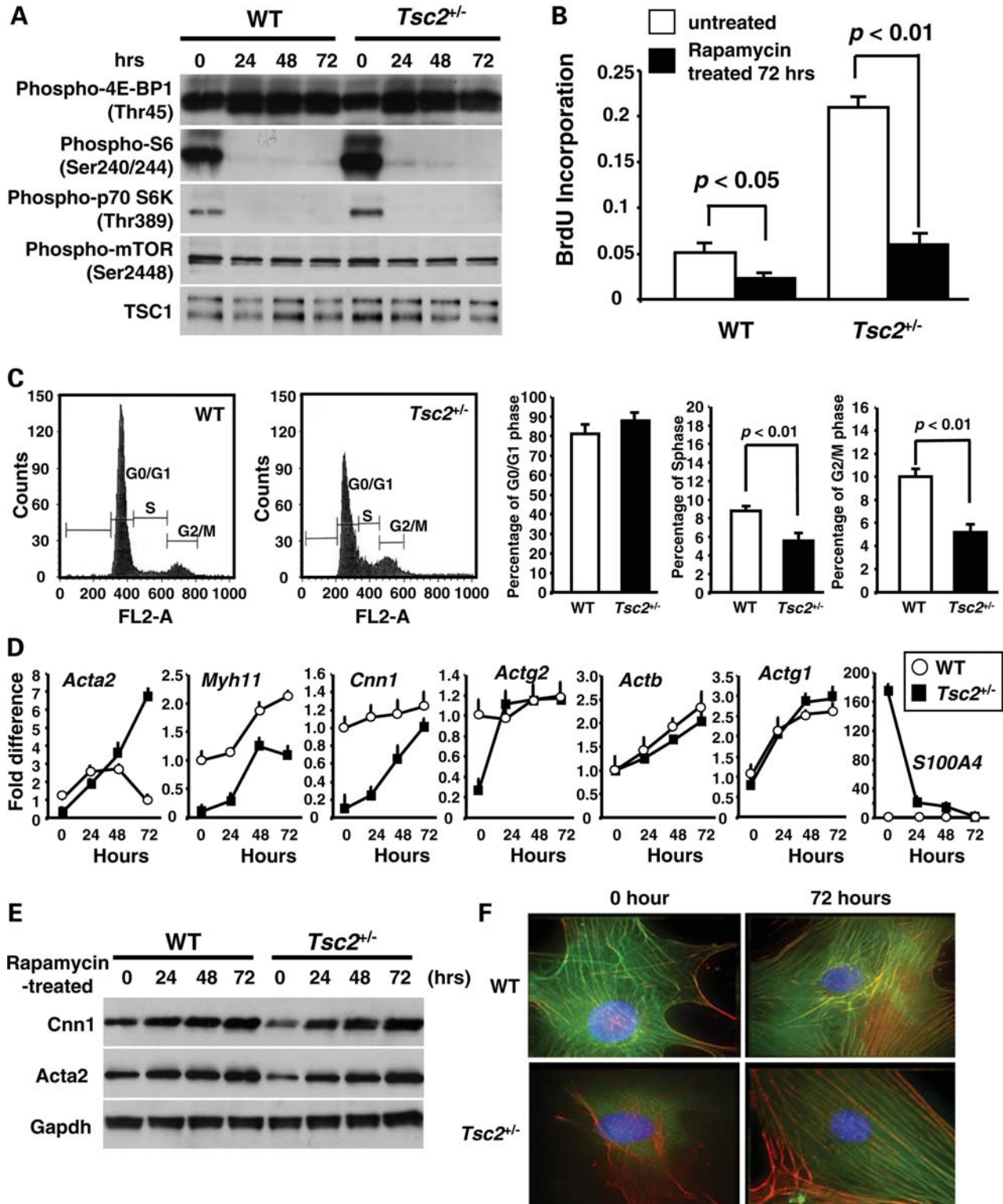


Figure 3. Phenotypic abnormalities in *Tsc2*^{+/-} SMCs are reversed by blocking mTOR signaling with rapamycin treatment. (A) Rapamycin treatment inhibited the phosphorylation of pS6 and p70 S6K in both mutant and WT cells. (B) BrdU assay demonstrates that rapamycin significantly inhibits SMC proliferation, especially the SMCs explanted from *Tsc2*^{+/-} aorta. (C) SMC cell counts by FACS analysis demonstrate that the number of *Tsc2*^{+/-} SMCs in G0/G1 phase is decreased and cells in S and G2/M phases increased compared with WT SMCs. Quantitative assessment of the percentage of SMCs at G0/G1, S and G2/M phases after treatment with rapamycin indicates that rapamycin induces cell cycle arrest at G0/G1 phase. Data are reported as means ± SD of three independent experiments. (D) qPCR analysis of mRNA isolated from SMCs from WT and *Tsc2*^{+/-} aorta indicates that expression of SMC contractile genes (*Acta2*, *Cnn1*, *Myh11*, *Actg2*) significantly increases after treatment with rapamycin, and expression of *S100A4* significantly decreases. RNA levels were normalized to *Gapdh*. (E) Protein levels of SMC contractile proteins, *Cnn1* and *Acta2*, in SMCs explanted from control and *Tsc2*^{+/-} after treated with rapamycin. Protein levels were normalized to *Gapdh*. (F) Immunofluorescence analysis of α-actin and stress fibers in cultured SMCs from control and *Tsc2*^{+/-} aorta. SMC nuclei were counterstained with DAPI (blue). Magnification × 600.

with increased expression and protein levels of contractile proteins. qPCR of *Acta2*, *Myh11*, *Cnn1* and *Actg2* confirmed that the gene expression of these contractile proteins progressively increased after the treatment with rapamycin, rising to levels similar to controls (Fig. 3D). A similar increase in these contractile proteins was found by immunoblot analysis. Although *Acta2* mRNA expression rose for 48 h, then declined at 72 h, the protein levels continued to accumulate (Fig. 3D and E). Interestingly, expression of cytoskeletal genes, *Actb* and *Actg1*, increased in response to rapamycin in both the WT and mutant SMCs. After treatment with rapamycin within 24 h, *S100A4* decreased significantly to levels equal with WT levels after 72 h (Fig. 3D).

Immunofluorescence using an antibody directed against α -actin was used to confirm that rapamycin treatment of *Tsc2*^{+/-} SMCs promoted assembly of contractile filaments. α -Actin is incorporated into actin filaments of the contractile unit in vascular SMCs, whereas β -actin is found in the actin filaments of the cytoskeleton (27). Antibodies specific for α -actin were used (green fluorescence) and all actin filaments, including β -actin-containing cytoskeleton filaments (stress fibers), were visualized with phalloidin (red fluorescence). WT SMCs showed organized stress fibers containing α -actin spanning the cell body, whereas *Tsc2*^{+/-} SMCs showed normal actin stress fiber formation but diminished staining for α -actin (Fig. 3F and Supplementary Material, Fig. S1). After treatment with rapamycin, *Tsc2*^{+/-} SMCs showed well-organized stress fibers spanning the cell body containing α -actin similar to the WT SMCs. Therefore, rapamycin reversed the de-differentiated phenotype of the *Tsc2*^{+/-} SMCs, specifically decreasing proliferation and increasing expression and assembly of contractile proteins.

***Tsc2*^{+/-} mice have increased neointima formation and vessel lumen occlusion in response to arterial injury**

Initial assessment of the ascending, descending and abdominal aorta showed normal aortic architecture with intact layers of elastin lamellae and SMCs located between the lamellae in both the WT and *Tsc2*^{+/-} mice (data not shown). To examine SMC proliferation *in vivo*, we used an established vascular injury protocol (28); the left common carotid artery was ligated near its bifurcation in WT and *Tsc2*^{+/-} mice and the arteries were harvested at 21 days. Histological examination of the uninjured carotid arteries from WT and *Tsc2*^{+/-} mice demonstrated the absence of a neointima formation and no structural differences in vessel architecture (Fig. 4A). Detailed morphometric analysis revealed that the injured arteries isolated from *Tsc2*^{+/-} mice had a 4-fold increase in neointimal area compared with WT controls (Fig. 4B). The intimal/medial (I/M) ratios of the injured arteries in *Tsc2*^{+/-} mice were 3-fold higher than those of WT controls. Furthermore, *Tsc2*^{+/-} mice had a 5-fold increase in percent lumen stenosis in response to injury compared with that of WT mice, all data supporting increased proliferation of the mutant SMCs *in vivo*.

We also tested whether administration of rapamycin could inhibit neointima formation in *Tsc2*^{+/-} mice after arterial injury. Twenty-one days after carotid artery injury, *Tsc2*^{+/-} mice with rapamycin treatment showed a 4-fold reduction in

I/M ratio compared with those treated with vehicle treatment (Fig. 4C and D).

α -Elastin peptides activate Rho signaling and decrease *Tsc2*^{+/-} SMC proliferation

Despite the increased proliferation of descending aortic *Tsc2*^{+/-} SMCs, the aortic pathology of *Tsc2*^{+/-} mice failed to demonstrate any evidence of increased proliferation *in vivo*. Since the proliferation of elastin-deficient SMCs (*Eln*^{-/-} SMCs) is decreased with the exposure to tropoelastin or acid hydrolyzed elastin fibers (α -elastin) (29), we sought to determine whether α -elastin would have a similar effect on suppressing *Tsc2*^{+/-} SMC proliferation. When SMCs were treated for 72 h with varying doses of soluble α -elastin, proliferation of the WT SMCs was unaffected, whereas the cell proliferation of *Tsc2*^{+/-} SMCs was markedly reduced in a dose-dependent manner (Fig. 5A). To determine whether the decreased proliferation in mutant SMCs with α -elastin exposure was due to apoptosis, flow cytometric analysis using dual staining with propidium iodide (PI) and FITC-conjugated annexin V was performed after SMCs were treated with different doses of α -elastin. No significant increase in apoptosis was found in either the WT or *Tsc2*^{+/-} SMCs (data not shown).

Previous studies have indicated that elastin regulates SMC proliferation via a G-protein-coupled signaling pathway (29). Incubation of the *Tsc2*^{+/-} SMCs with a specific Rho kinase inhibitor (Y27632) blocked the α -elastin-induced decrease in cell proliferation (Fig. 5A). Levels of p27^{kip1} have been previously implicated controlling proliferation in *Tsc* mutant mouse embryonic fibroblasts and astrocytes (30). We found that the mutant SMCs had diminished levels of p27^{kip1} compared with WT SMCs at baseline, and p27^{kip1} levels increased in mutant SMCs with increasing amounts of α -elastin peptide (Fig. 5B). α -Elastin treatment of *Tsc2*^{+/-} SMCs was also found to inhibit mTORC1-p70S6 pathway signaling as evident by decreased phosphorylation of mTOR and p70S6K, a previously undescribed effect of α -elastin binding. Despite the decrease in proliferation, exposure to α -elastin did not alter the levels of *Acta2* or *Cnn1* in the *Tsc2*^{+/-} SMCs. Therefore, α -elastin binding to *Tsc2*^{+/-} SMCs increases p27^{kip1} levels, inhibits mTOR signaling and decreases proliferation but fails to induce expression of contractile proteins.

DISCUSSION

This study is the first to examine the etiology of vascular pathology associated with *TSC2* mutations. The aneurysm-associated pathology in TSC patients demonstrated subintimal proliferation of SMCs, suggesting increased SMC proliferation contributed to the formation of these aneurysms. We confirmed a thoracoabdominal aortic aneurysm associated with subintimal SMC proliferation in a child with a *TSC2* mutation. We demonstrated that the activation of mTORC1 signaling occurs in aortic SMCs with loss of only one allele of *Tsc2* and leads to de-differentiation of SMCs characterized by increased proliferation and decreased expression of contractile proteins. Rapamycin treatment effectively reverses

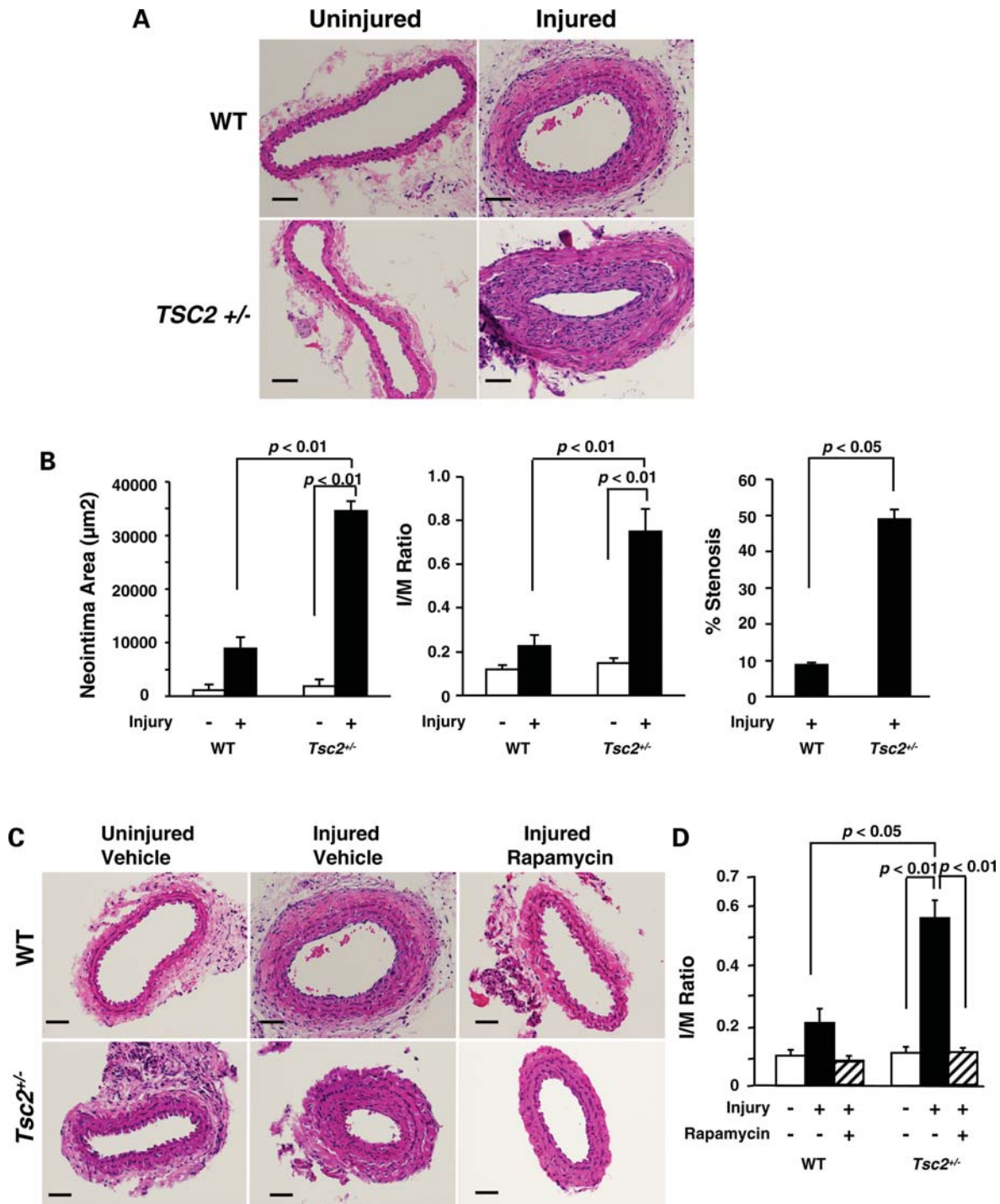


Figure 4. Histological and morphometric analysis of injured carotid arteries from WT and *Tsc2*^{+/-} mice. (A) Representative photomicrographs of carotid arteries from WT (top panels) and *Tsc2*^{+/-} (bottom panels) mice stained with H&E for 21 days following no injury (left panels) or injury (right panels). Scale bars represent 50 µm. Results are representative of seven independent experiments. (B) Neointima area of uninjured and injured carotid artery cross-sections from WT and *Tsc2*^{+/-} mice. Data represent mean neointima area of seven cross-sections ± SD, n = 7. For *Tsc2*^{+/-} uninjured versus injured, P < 0.01, and for WT injured versus *Tsc2*^{+/-} injured, P < 0.01. I/M ratio of uninjured and injured carotid artery cross-sections from WT and *Tsc2*^{+/-} mice. Data represent mean I/M ratio of seven cross-sections ± SD, n = 7. For *Tsc2*^{+/-} uninjured versus injured, P < 0.01, and for WT injured versus *Tsc2*^{+/-} injured, P < 0.01. Percentage of carotid artery stenosis 21 days following injury in WT and *Tsc2*^{+/-} mice. Data represent mean percent stenosis of seven cross-sections ± SD, n = 7, P < 0.05. (C) Representative photomicrographs of H&E-stained carotid arteries from WT (top panels) and *Tsc2*^{+/-} (bottom panels) mice 21 days following no injury and vehicle treatment (left panels), injury and vehicle treatment (middle panels) or injury and rapamycin treatment (right panels). Scale bars represent 50 µm. Results are representative of seven independent experiments. (D) I/M ratio of injured carotid artery cross-sections from vehicle and rapamycin-treated WT and *Tsc2*^{+/-} mice. Data represent mean I/M ratio of seven cross-sections ± SD, n = 7 mice. For *Tsc2*^{+/-} uninjured versus injured with vehicle treatment, P < 0.01; for *Tsc2*^{+/-} injured with vehicle versus injured with rapamycin treatment, P < 0.01; for WT injured with vehicle treatment versus *Tsc2*^{+/-} injured with vehicle treatment, P < 0.05.

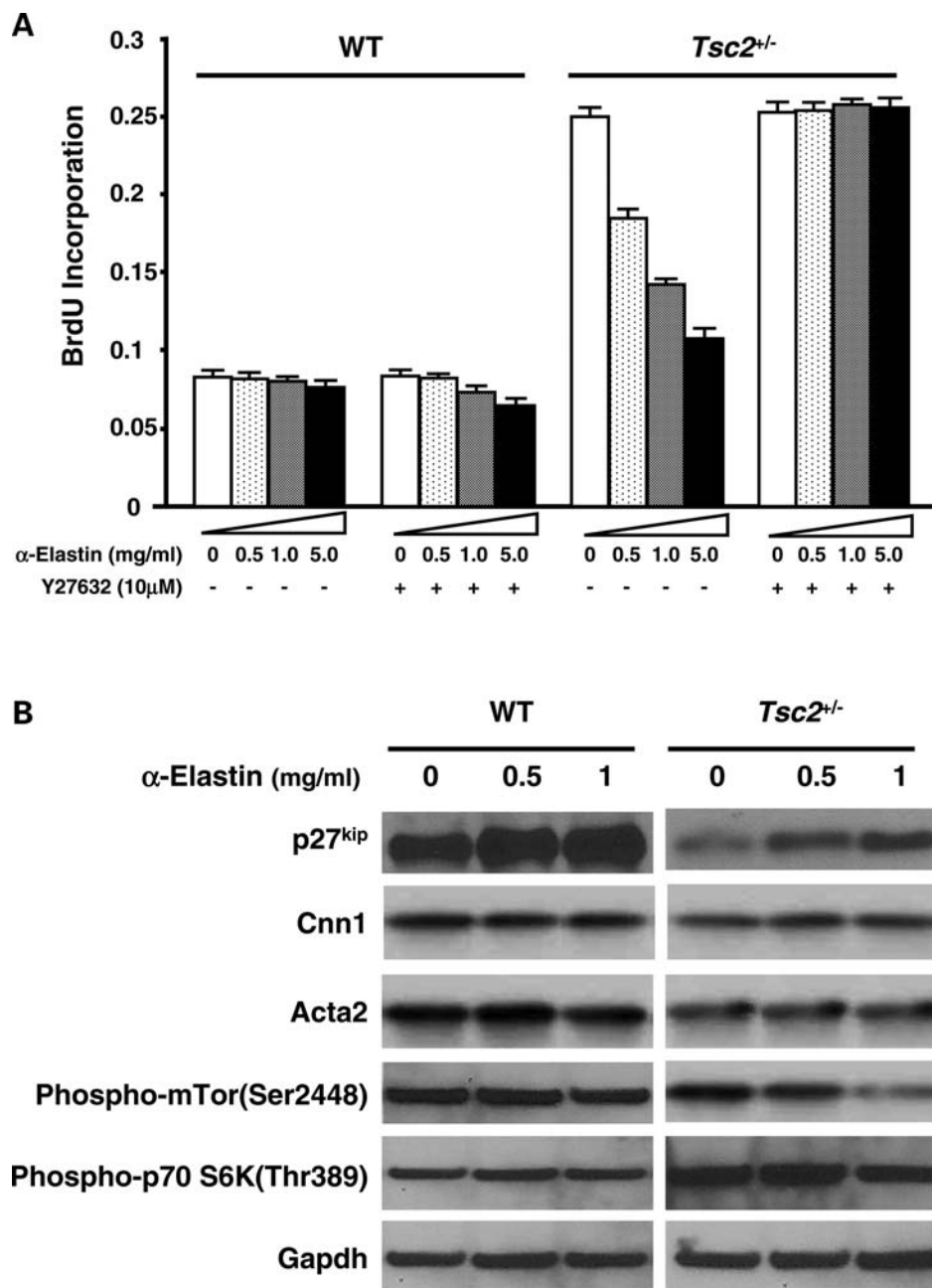


Figure 5. Effect of α -elastin exposure on cell proliferation and protein levels in $Tsc2^{+/-}$ SMCs. (A) SMCs explanted from WT and $Tsc2^{+/-}$ mice were cultured at α -elastin concentration of 0, 0.5, 1 and 5 mg/ml, respectively, for 72 h. BrdU assay demonstrated that proliferation of $Tsc2^{+/-}$ SMCs was inhibited in a dose-dependent manner. A specific Rho inhibitor (Y27632) could prevent the reduction of $Tsc2^{+/-}$ SMC proliferation by α -elastin. (B) Western blot assay demonstrated that α -elastin-treated $Tsc2^{+/-}$ SMCs increased expression level of p27^{kip1}, inhibited mTOR signaling and decreased SMC proliferation. In addition, α -elastin did not alter expression level of contractile proteins in $Tsc2^{+/-}$ SMCs.

the proliferation and de-differentiation of $Tsc2^{+/-}$ SMCs *in vitro* and *in vivo*, providing evidence that the effect of $Tsc2$ deficiency on vascular SMCs is primarily driven by increased mTORC1 signaling. It has previously been shown that in control SMCs, inhibition of mTORC1 using rapamycin promotes differentiation through the activation of the Akt pathway and the induction of SMC contractile protein expression (19). The effectiveness of rapamycin *in vivo* is illustrated by the success of rapamycin-eluting stents in pre-

venting stent occlusion due to SMC proliferation (31). These clinical studies and the data presented here suggest a potential therapeutic use of rapamycin or rapamycin-eluting stents for the treatment of aortic aneurysms and potentially other vascular disease in TSC patients.

Elastin, the predominant extracellular protein in major arteries, is synthesized and secreted as a monomer, tropoelastin, which is crosslinked and organized into elastin polymers that form the concentric lamellae in the medial layer of arteries (32,33). The layers

of elastin lamellae alternate with layers of SMCs in elastic arteries to form a unique structure designed to absorb hemodynamic forces. A role of elastin in controlling SMC proliferation was first suggested by the observation that loss-of-function mutations in one elastin allele lead to supraaortic stenosis, a vascular disease characterized by fibrocellular SMC proliferation in the aorta and other arteries (34). Further *in vitro* studies confirmed that elastin deficiency increases SMC proliferation rates by demonstrating increased proliferation of SMCs explanted from the *Eln*^{-/-} mouse (29). Addition of tropoelastin or α -elastin to these cells decreases SMC proliferation via a G-protein-coupled signaling pathway. The decreased proliferation occurs without the induction of the expression of α -actin, a major component of the SMC contractile unit. Our data indicate that exposure to α -elastin peptides also decreases proliferation rates of *Tsc2*^{+/-} cells, a change associated with increased p27^{kip1} protein levels, suggesting that the anti-proliferative effects of α -elastin binding are mediated, in part, through p27^{kip1}. Elastin fragments also decrease mTOR signaling in the *Tsc2*^{+/-} SMCs through an undetermined mechanism. The observation that α -elastin binding decreases SMC proliferation through Rho kinase signaling is counter to the literature on Rho kinase signaling and SMC proliferation. For many years, it has been recognized that the specific Rho kinase inhibitor, Y27632, suppresses both mitogen-induced DNA synthesis in SMCs and neointimal proliferation after balloon-injured carotid arteries in a rat model (35). The suppression of SMC proliferation with Y27632 is associated with increased levels of p27^{kip1}. As mentioned earlier, previous studies have shown that elastin binding decreases the proliferation rates in *Eln*^{-/-} SMCs through Rho kinase signaling. Although elastin had no effect on WT SMC proliferation rates, elastin suppressed proliferation in the *Tsc2*^{+/-} aortic SMCs, associated with increased p27^{kip1} levels and decreased mTOR signaling, and a Rho kinase inhibitor blocked these effects. These results suggest the possibility that elastin binding suppresses SMC proliferation resulting from an underlying genetic mutation (e.g. *Eln* or *Tsc2* deficiency) through Rho kinase signaling pathway, leading to increased p27^{kip1} levels.

SMCs in the ascending aorta are derived from the neural crest cells, whereas SMCs in the descending and abdominal aortas originate from mesodermal cells (22,36,37). Aortic aneurysms in TSC children involve almost exclusively the descending and abdominal aorta. Pathological findings of the TSC-associated aortic aneurysms are similar to the pathology in the patient reported here, including the loss of elastic fibers, disruption of the organized structure of the aortic media and nodular proliferation of SMCs (38–40). Our data indicate that loss of *Tsc2* has a more pronounced effect on mesodermal-derived SMCs than neural crest-derived SMCs, and this increased proliferative potential and decreased expression of contractile proteins of the descending aortic SMCs may contribute to preferential involvement of the descending aorta in this disorder. The low penetrance of this aortic complication in TSC patients raises the possibility that loss of heterozygosity (LOH) for the *Tsc2* allele is required for the increased proliferation of the SMCs associated with the aortic aneurysm formation. It is important to note that the *Tsc2*^{+/-} SMCs demonstrated increased proliferation *in vitro* without evidence of LOH. In addition, the consistent increase in SMC proliferation in response to carotid injury

in the *Tsc2*^{+/-} mouse implies that LOH is not required for the *in vivo* increase in SMC proliferative response when compared with control mice. Further studies will determine whether LOH is involved in the aortic aneurysm formation in TSC patients. At the same time, aortic imaging of a cohort of TSC children will determine whether aortic dilatation is present frequently in TSC children but resolves and does not progress to aneurysm formation.

The vascular disease and increased SMC proliferation associated with *TSC2* mutations have similarities to vascular disease in patients with neurofibromatosis type I (NF1) (41,42). Similar to TSC, one of the less studied and most poorly recognized complications of NF1 is the vasculopathy that affects arteries ranging in size from the proximal aorta to small arteries and may produce vascular diseases, including aneurysms. Similar to the pathological lesions observed in TSC patients, the lesions in the small vessels of NF1 patients are characterized by medial and intimal SMC hyperplasia (43,44). NF1 is due to heterozygous mutations in the *NF1* gene, which encodes neurofibromin, a tumor-suppressor that functions in part as a negative regulator of RAS signaling (45). In the mouse, partial or complete loss of neurofibromin expression in SMCs leads to marked SMC intimal hyperproliferation in response to vascular injury (46,47). Similar to the *Tsc2*^{+/-} mutant SMCs, SMCs explanted from the mice lacking or deficient in *NF1* expression displayed increased proliferation *in vitro* compared with WT SMCs (46,48).

In summary, SMCs harboring loss of one allele of *Tsc2* have a significantly altered phenotype of increased proliferation and decreased contractile protein expression when compared with WT SMCs. Rapamycin effectively reversed the abnormal SMC phenotype, whereas binding to elastin peptides reversed the proliferation but failed to induce expression of contractile proteins. On the basis of these data, we propose that *Tsc2*^{+/-} mutant SMCs proliferate normally when associated with elastin fibers but may fail to fully express the repertoire of proteins required for normal contractile function. This defect in SMCs is more pronounced in the descending aorta than the ascending most likely due to different cell lineage origins of the SMCs in these two vascular beds. It is also important to note that the relative ratios of elastin to collagen progressively decrease from the ascending aorta to the abdominal aorta (32), and this may contribute to the unique presentation of the disease primarily in the abdominal aorta in TSC patients. This decrease in contractile proteins in the SMCs may lead to decreased ability to contract with each pulse wave and contribute to aneurysm formation, consistent with a pathway previously suggested for ascending aneurysms formation (49). Future studies will further delineate the molecular pathogenesis of these aneurysms in TSC patients, information that has the potential to contribute to our understanding of the pathogenesis of the most common type of aortic aneurysm, abdominal aortic aneurysms.

MATERIALS AND METHODS

Patient material and mutation analysis

The Institutional Review Board at the University of Texas Health Science Center at Houston (UTHSCH) approved this study. All patient material and records were collected after

approved consent was signed. Analysis of the *TSC1* and *TSC2* genes was performed by Athena Diagnostics, Inc.

Animals

We used 6- to 8-week-old WT and age-matched *Tsc2*^{+/-} mice, which contain a deletion of *Tsc2* involving exons 2 through 4 (20,21). The WT and heterozygous mice are of mixed 129×1/SvJ and C57BL/6 background. The animals were cared for according to the NIH Guide for the Care and Use of Laboratory Animals. Ketamine–xylazine was used to anesthetize mice prior to euthanasia. The thorax was opened beneath the xiphoid process. An incision was made in the right atrium to provide an outlet for blood and perfusate. The left ventricle was then punctured with a 22-gauge needle aimed at the direction of the left ventricular outflow tract. The needle was attached to a perfusion system that provided initial perfusion with normal saline at 100 mmHg. This continued until outflow from the right atrial incision was clear and the liver appeared blanched (50). At this time point, both WT and *Tsc2*^{+/-} mice were divided into two groups. Half of the mice were perfused with 10% formalin in phosphate buffer saline (PBS) at 100 mmHg for 3 min. The aorta was carefully harvested from its root to the renal arteries. The excised aorta was fixed in 10% neutral-buffered formalin and processed for routine paraffin embedding. For another half of mice, whole aortas were collected under sterile conditions and put into biopsy medium [Waymouth's medium (Invitrogen) supplemented with 100 U/ml of penicillin, 100 µg/ml of streptomycin, 250 ng/ml of amphotericin, 2.5 mM L-glutamine, 1 mM MEM non-essential amino acids, 100 mM HEPES buffer and sodium bicarbonate].

Carotid artery injury and rapamycin treatment

Fourteen 8-week-old WT and 14 age-matched *Tsc2*^{+/-} mice were anesthetized by intraperitoneal injection of 2.5% avertin. The left common carotid artery was ligated near its bifurcation with the use of 5-0 silk. The wound was sutured. Animal survival was >95%. For morphological analysis, animals were perfused with normal saline and fixed with 10% phosphate-buffered formalin at physiological pressure for 3 min. Left and right carotid arteries were removed in block, further fixed for 16 h and paraffin-embedded without further dissection. Because lesion thickness varies longitudinally, the entire length of the left and right carotid arteries was sectioned and examined for identification of the apex of the lesion, which displays the smallest lumen. For morphometric analyses, images of hematoxylin and eosin (H&E)-stained cross-sections of injured and control arteries were analyzed using Image J. Perimeters of the lumen, IEL and external elastic lamina (EEL) were obtained by tracing the contours on digitized images. Intimal thickness (distance between lumen and IEL) and medial thickness (distance between IEL and EEL) were automatically calculated. Percent lumen stenosis was calculated as: (intima area/IEL area) × 100. For the rapamycin treatment, 2 mg/kg rapamycin (A.G. Scientific, Inc.) in dimethyl sulfoxide (DMSO) or DMSO alone (vehicle) was administered once intraperitoneally at 4 h following injury and continued for 2 weeks by 2 mg/kg daily.

Cell culture

Ascending aorta/arch and descending aortas were separated after the origin of the left subclavian artery. Each part of the aorta was successively washed with 70% ethanol, PBS and aortic biopsy medium. A scalpel was used to remove the endothelial cell layers and the adventitia, and the remaining medial layer of aorta from mutant and WT mice was chopped into small pieces and put to digestion overnight for 16 h in 5 ml of aortic biopsy medium supplemented with 0.1 mg/ml of collagenase type I, 0.01875 mg/ml of elastase type I and 0.0250 mg/ml of soybean trypsin inhibitor. At the end of incubation, the digestion was stopped with 2.5 ml of fetal bovine serum (FBS) and 2.5 ml of complete SMC medium [SmBM from Lonza supplemented with 20% FBS, 100 U/ml of penicillin, 100 µg/ml of streptomycin, 250 ng/ml of amphotericin, 0.5 ml of insulin, 1.0 ml of rhEGF, 0.5 ml of rhFGF, 2 mmol/l of L-glutamine, 20 mmol/l of HEPES, 1 mmol/l of sodium pyruvate (Clonetics)] (46). Cells and tissue were spun down, washed once with complete SMC medium, spun down again, resuspended in complete SMC medium and seeded into flasks for further experiments. The identity of these cells as SMCs was verified by staining for smooth muscle α -actin (mouse monoclonal antibody; Sigma) at each passage (>95% of cells stained positive for smooth muscle α -actin). SMCs were cultured in complete SMC medium in a 37°C, 5% CO₂-humidified incubator. Four independent cell lines were explanted from WT mice and mutant mice, using three mice in each group. The results presented are representative of duplicate experiments done on these SMCs using matched passage levels between WT and mutant SMCs, with all studies done on SMCs at less than passage 5.

For rapamycin treatment, SMCs were plated at a density of 100 cells/mm². After 8 h incubation in serum-containing media as noted earlier, the cells were serum-starved for 24 h for cell cycle synchronization. The cells were treated with 20 nmol/l of rapamycin (MP Biomedicals) or with DMSO (vehicle control) in SmBM plus 5% FBS for 24, 48, 72 h. The medium was refreshed every 24 h. For α -elastin and Rho kinase inhibitor treatment, SMCs were seeded in a 96-well tissue culture plate at a density of 20 000 cells/well for 8 h in serum-containing media as noted earlier. The cells were serum-starved for 24 h for cell cycle synchronization. Cells were then cultured with SmBM containing 5% FBS plus α -elastin (at concentration of 0, 0.5, 1 and 5 mg/ml, respectively) in the presence or absence of Rho kinase inhibitor (10 µM, InSolution™ Rho Kinase Inhibitor, Calbiochem) for the next 72 h.

Histological and immunohistochemical studies

The excised aorta was fixed in 10% neutral-buffered formalin and processed for routine paraffin embedding. Aorta tissue cross-sections (6 µm) were stained with H&E in a standard manner. Immunohistochemical staining was performed using an avidin–biotin complex system. Sections were de-paraffinized and rehydrated by immersing in xylenes and graded alcohol series, followed by heat-induced epitope retrieval using 10 mM citrate buffer, pH 6.0. Following antigen recovery, aortic tissue slides were incubated for 1 h with

blocking reagent. The sections were incubated overnight at 4°C with mouse-monoclonal α -smooth muscle actin (α -SMA) antibody (Sigma, St Louis, MO, USA). After washing in PBS and incubation with a biotinylated secondary antibody, the slides were treated with peroxidase-conjugated biotin-avidin complex (Vectastain ABC-AP Kit, Vector Laboratories, Burlingame, CA, USA). Finally, peroxidase was revealed by immersion in alkaline phosphatase substrate solution (Vector Red Alkaline Phosphatase Substrate Kit, Vector Laboratories). Slides were counterstained with hematoxylin.

Immunofluorescence of SMCs

To analyze the contractile protein expression and stress fiber formation in SMCs, cells were immunofluorescently stained for α -SMA and phalloidin. After cells reached confluence, they were seeded onto coverslips in six-well plates with the density of 13 cells/mm² for 24 h prior to serum-starvation. After 24 h serum-starvation, cells for baseline were fixed, and remains were stimulated with 20 nmol/l of rapamycin in SmBM plus 5% FBS for 72 h. The media was refreshed every 24 h. Cells were fixed with 4% paraformaldehyde in 0.1 M phosphate buffer for 10 min and washed three times with cold PBS prior to permeabilization. Permeabilization and blocking of nonspecific binding sites were performed in PBS containing 1% bovine serum albumin (BSA) and 0.5% Tween20. For phalloidin staining, coverslips were incubated with Texas Red-labeled phalloidin (1:40 in blocking solution) (Molecular Probes, Eugene, OR, USA) for 30 min at room temperature and washed three times with PBS. Coverslips were then treated with antibody to α -SMA (1:100) for 1 h followed by fluorescein isothiocyanate-conjugated secondary antibody (1:200) for 1 h at room temperature. Nuclei were counterstained with DAPI (Vector Laboratories), and then randomly chosen fields on each coverslip were imaged by laser scanning fluorescence microscopy (OLYMPUS IX70) and analyzed with a deconvolution system (DeltaVision Deconvolution System, Applied Precision, Issaquah, WA, USA).

Cell proliferation assay

DNA incorporation into proliferating cells was quantified using a BrdU Cell Proliferation Kit (Chemicon, Cat.2752). Briefly, SMCs were seeded in 96-well plates (20 000 cells/well) and grown for 8 h in SmBM containing 20% FBS. The cells were serum-starved for 24 h for cell cycle synchronization. Subsequently, the cells were treated with DMSO or rapamycin for an additional 72 h. The media were refreshed every 24 h. Then, BrdU was added to the culture medium. BrdU incorporation was quantified by ELISA according to the manufacturer's instructions.

FACS analysis

Cell cycle was determined by flow cytometry in PI-stained cells. At each time point, the cells were serum-starved for 24 h for cell cycle synchronization. Then, cells were digested with trypsin-EDTA from culture plates. Cells (2×10^6) were collected by low-speed centrifugation, washed with cold PBS,

recollected by centrifugation, fixed with 70% ethanol at room temperature for at least 30 min, then stored at -20°C overnight. After washing twice, cells were stained with 50 μ g/ml of PI, and 10 mg/ml of RNase A (Bachem California, Torrance, CA, USA) was added 30 min before flow cytometry analysis. Red fluorescence was measured with a FACScan (Becton Dickinson, San Jose, CA, USA). DNA content and cell cycle profiles were analyzed to determine fractions of the population in each phase of the cell cycle (G0/G1, S, G2/M).

SDS-PAGE and western blotting analysis

Cells were washed twice with ice-cold PBS and lysed in RIPA buffer (50 mM of Tris, pH 7.5, 150 mM of NaCl, 1% NP-40, 0.5% sodium deoxycholate and 0.1% SDS) supplemented with protease inhibitor cocktail (Sigma) and phosphatase inhibitor cocktail (Sigma). Protein concentration was determined by the Bio-Rad protein assay. Total cell lysates (10 μ g) were separated by SDS-PAGE with Tris-HCl gel (Ready Gel, Bio-Rad, Hercules, CA, USA), followed by transfer to polyvinylidene difluoride membranes (Immobilon-P, Millipore, Bedford, MA, USA). Membranes were incubated in blocking buffer (5% nonfat milk in T-PBS) for 1 h and immunoblotted with primary antibody diluted in 5% BSA (Sigma). Membranes were probed with horseradish peroxidase-conjugated secondary antibody (Jackson ImmunoResearch Laboratories, West Grove, PA, USA). Western blots were visualized by the enhanced chemiluminescence technique (Amersham ECL Western Blotting Detection Reagents, GE Healthcare, Piscataway, NJ, USA). Primary antibodies include anti-TSC2, anti-TSC1, anti- α -tubulin (11H10), anti-mTOR (7C10), anti-Phospho-mTOR (Ser2448), anti-p70 S6 Kinase, anti-Phospho-p70 S6 Kinase (Thr389), anti-S6 (5G10), anti-Phospho S6 (Ser240/244) (all from Cell Signaling Technology), anti-Phospho-4E-BP1 (Thr45)(from Signalway Antibody), anti-SM myosin, anti- α -SMA, anti-calponin, anti-GAPDH (all from Sigma).

qPCR analysis

Total cellular RNA was extracted using TRI reagent (Sigma) according to the manufacturer's protocol. qPCR analysis was carried out using pre-designed TaqMan assays from Applied Biosystems using manufacturer's protocols and reagents and run on an ABI Prism 7700 Sequence Detection System (Applied Biosystems).

Statistical analysis

All values are expressed as means \pm SD. Statistical differences between *Tsc2*^{+/-} cells and controls were analyzed by a Student's *t*-test. Morphometric analysis of carotid artery was done by one-way ANOVA. Differences were considered statistically significant at values of *P* < 0.05. Data for cell culture experiments represent three experiments in triplicates using separate cultures.

SUPPLEMENTARY MATERIAL

Supplementary Material is available at *HMG* online.

ACKNOWLEDGEMENTS

We would like to thank Dr Steven P. Sparagana, MD, pediatric neurologist at Texas Scottish Rite Hospital for Children, for assistance with the genetic testing.

Conflict of Interest statement. None declared.

FUNDING

The following sources provided funding for these studies: P50HL083794-01 (D.M.M.), RO1 HL62594 (D.M.M.), NIH/NINDS RO1 NS060804 (M.J.G.) and the Vivian L. Smith Foundation.

REFERENCES

- Osborne, J.P., Fryer, A. and Webb, D. (1991) Epidemiology of tuberous sclerosis. *Ann. N. Y. Acad. Sci.*, **615**, 125–127.
- van Slegtenhorst, M., de Hoogt, R., Hermans, C., Nellist, M., Janssen, B., Verhoef, S., Lindhout, D., van den, O.A., Halley, D., Young, J. *et al.* (1997) Identification of the tuberous sclerosis gene TSC1 on chromosome 9q34. *Science*, **277**, 805–808.
- The European Chromosome 16 Tuberous Sclerosis Consortium (1993) Identification and characterization of the tuberous sclerosis gene on chromosome 16. *Cell*, **75**, 1305–1315.
- Wienecke, R., Konig, A. and DeClue, J.E. (1995) Identification of tuberin, the tuberous sclerosis-2 product. Tuberin possesses specific Rap1GAP activity. *J. Biol. Chem.*, **270**, 16409–16414.
- Xiao, G.H., Shoarinejad, F., Jin, F., Golemis, E.A. and Yeung, R.S. (1997) The tuberous sclerosis 2 gene product, tuberin, functions as a Rab5 GTPase activating protein (GAP) in modulating endocytosis. *J. Biol. Chem.*, **272**, 6097–6100.
- Maheshwar, M.M., Cheadle, J.P., Jones, A.C., Myring, J., Fryer, A.E., Harris, P.C. and Sampson, J.R. (1997) The GAP-related domain of tuberin, the product of the TSC2 gene, is a target for missense mutations in tuberous sclerosis. *Hum. Mol. Genet.*, **6**, 1991–1996.
- Zhang, Y., Gao, X., Saucedo, L.J., Ru, B., Edgar, B.A. and Pan, D. (2003) Rheb is a direct target of the tuberous sclerosis tumour suppressor proteins. *Nat. Cell Biol.*, **5**, 578–581.
- Inoki, K., Li, Y., Xu, T. and Guan, K.L. (2003) Rheb GTPase is a direct target of TSC2 GAP activity and regulates mTOR signaling. *Genes Dev.*, **17**, 1829–1834.
- Tee, A.R., Manning, B.D., Roux, P.P., Cantley, L.C. and Blenis, J. (2003) Tuberous sclerosis complex gene products, Tuberin and Hamartin, control mTOR signaling by acting as a GTPase-activating protein complex toward Rheb. *Curr. Biol.*, **13**, 1259–1268.
- Jozwiak, J., Jozwiak, S., Grzela, T. and Lazarczyk, M. (2005) Positive and negative regulation of TSC2 activity and its effects on downstream effectors of the mTOR pathway. *Neuromolecular Med.*, **7**, 287–296.
- Fingar, D.C., Salama, S., Tsou, C., Harlow, E. and Blenis, J. (2002) Mammalian cell size is controlled by mTOR and its downstream targets S6K1 and 4E-BP1/eIF4E. *Genes Dev.*, **16**, 1472–1487.
- Fingar, D.C., Richardson, C.J., Tee, A.R., Cheatham, L., Tsou, C. and Blenis, J. (2004) mTOR controls cell cycle progression through its cell growth effectors S6K1 and 4E-BP1/eukaryotic translation initiation factor 4E. *Mol. Cell Biol.*, **24**, 200–216.
- Lavocat, M.P., Teyssier, G., Allard, D., Tronchet, M. and Freycon, F. (1992) Abdominal aortic aneurysm and Bourneville's tuberous sclerosis. *Pediatrics*, **47**, 517–519.
- Freycon, F., Mollard, P., Hermier, M., Guibaud, P., Chazalotte, J.P., Weill, B., Flattot, M. and Jeune, M. (1971) Abdominal aorta aneurysm during Bourneville's tuberous sclerosis. *Pediatrics*, **26**, 421–427.
- Larbre, F., Loire, R., Guibaud, P., Lauras, B. and Weill, B. (1971) Clinical and anatomical case of an aortic aneurysm in the course of Bourneville's tuberous sclerosis. *Arch. Fr. Pediatr.*, **28**, 975–984.
- Shepherd, C.W., Gomez, M.R., Lie, J.T. and Crowson, C.S. (1991) Causes of death in patients with tuberous sclerosis. *Mayo Clin. Proc.*, **66**, 792–796.
- Patino, B.E., Calderon-Colmenero, J., Buendia, A. and Juanico, A. (2005) Giant aortic aneurysm and rhabdomyomas in infant with tuberous sclerosis (case report). *Arch. Cardiol. Mex.*, **75**, 448–450.
- Martin, K.A., Rzuclidlo, E.M., Merenick, B.L., Fingar, D.C., Brown, D.J., Wagner, R.J. and Powell, R.J. (2004) The mTOR/p70 S6K1 pathway regulates vascular smooth muscle cell differentiation. *Am. J. Physiol. Cell Physiol.*, **286**, C507–C517.
- Martin, K.A., Merenick, B.L., Ding, M., Fetalvero, K.M., Rzuclidlo, E.M., Kozul, C.D., Brown, D.J., Chiu, H.Y., Shyu, M., Drapeau, B.L. *et al.* (2007) Rapamycin promotes vascular smooth muscle cell differentiation through insulin receptor substrate-1/phosphatidylinositol 3-kinase/Akt2 feedback signaling. *J. Biol. Chem.*, **282**, 36112–36120.
- Onda, H., Lueck, A., Marks, P.W., Warren, H.B. and Kwiatkowski, D.J. (1999) Tsc2(+/-) mice develop tumors in multiple sites that express p16 and are influenced by genetic background. *J. Clin. Invest.*, **104**, 687–695.
- Hernandez, O., Way, S., McKenna, J. III and Gambello, M.J. (2007) Generation of a conditional disruption of the Tsc2 gene. *Genesis*, **45**, 101–106.
- Majesky, M.W. (2007) Developmental basis of vascular smooth muscle diversity. *Arterioscler. Thromb. Vasc. Biol.*, **27**, 1248–1258.
- Gao, X., Zhang, Y., Arrazola, P., Hino, O., Kobayashi, T., Yeung, R.S., Ru, B. and Pan, D. (2002) Tsc tumour suppressor proteins antagonize amino-acid-TOR signalling. *Nat. Cell Biol.*, **4**, 699–704.
- Tee, A.R., Fingar, D.C., Manning, B.D., Kwiatkowski, D.J., Cantley, L.C. and Blenis, J. (2002) Tuberous sclerosis complex-1 and -2 gene products function together to inhibit mammalian target of rapamycin (mTOR)-mediated downstream signaling. *Proc. Natl Acad. Sci. USA*, **99**, 13571–13576.
- Brisset, A.C., Hao, H., Camenzind, E., Bacchetta, M., Geinoz, A., Sanchez, J.C., Chaponnier, C., Gabbiani, G. and Bochaton-Piallat, M.L. (2007) Intimal smooth muscle cells of porcine and human coronary artery express S100A4, a marker of the rhomboid phenotype *in vitro*. *Circ. Res.*, **100**, 1055–1062.
- Huang, S., Bjornsti, M.A. and Houghton, P.J. (2003) Rapamycins: mechanism of action and cellular resistance. *Cancer Biol. Ther.*, **2**, 222–232.
- Guo, D.C., Pannu, H., Papke, C.L., Yu, R.K., Avidan, N., Bourgeois, S., Estrera, A.L., Safi, H.J., Sparks, E., Amor, D. *et al.* (2007) Mutations in smooth muscle α -actin (*ACTA2*) lead to thoracic aortic aneurysms and dissections. *Nat. Genet.*, **39**, 1488–1493.
- Kumar, A. and Lindner, V. (1997) Remodeling with neointima formation in the mouse carotid artery after cessation of blood flow. *Arterioscler. Thromb. Vasc. Biol.*, **17**, 2238–2244.
- Karnik, S.K., Brooke, B.S., Bayes-Genis, A., Sorensen, L., Wythe, J.D., Schwartz, R.S., Keating, M.T. and Li, D.Y. (2003) A critical role for elastin signaling in vascular morphogenesis and disease. *Development*, **130**, 411–423.
- Uhlmann, E.J., Apicelli, A.J., Baldwin, R.L., Burke, S.P., Bajenaru, M.L., Onda, H., Kwiatkowski, D. and Gutmann, D.H. (2002) Heterozygosity for the tuberous sclerosis complex (TSC) gene products results in increased astrocyte numbers and decreased p27-Kip1 expression in TSC2^{+/-} cells. *Oncogene*, **21**, 4050–4059.
- Holmes, D.R. Jr, Leon, M.B., Moses, J.W., Popma, J.J., Cutlip, D., Fitzgerald, P.J., Brown, C., Fischell, T., Wong, S.C., Midei, M. *et al.* (2004) Analysis of 1-year clinical outcomes in the SIRIUS trial: a randomized trial of a sirolimus-eluting stent versus a standard stent in patients at high risk for coronary restenosis. *Circulation*, **109**, 634–640.
- Wolinsky, H. and Glagov, S. (1967) A lamellar unit of aortic medial structure and function in mammals. *Circ. Res.*, **20**, 99–111.
- Mecham, R.P. (1991) Elastin synthesis and fiber assembly. *Ann. N. Y. Acad. Sci.*, **624**, 137–146.
- Li, D.Y., Fauray, G., Taylor, D.G., Davis, E.C., Boyle, W.A., Mecham, R.P., Stenzel, P., Boak, B. and Keating, M.T. (1998) Novel arterial pathology in mice and humans hemizygous for elastin. *J. Clin. Invest.*, **102**, 1783–1787.

35. Sawada, N., Itoh, H., Ueyama, K., Yamashita, J., Doi, K., Chun, T.H., Inoue, M., Masatsugu, K., Saito, T., Fukunaga, Y. *et al.* (2000) Inhibition of rho-associated kinase results in suppression of neointimal formation of balloon-injured arteries. *Circulation*, **101**, 2030–2033.
36. Gittenberger-de Groot, A.C., DeRuiter, M.C., Bergwerff, M. and Poelmann, R.E. (1999) Smooth muscle cell origin and its relation to heterogeneity in development and disease. *Arterioscler. Thromb. Vasc. Biol.*, **19**, 1589–1594.
37. Bergwerff, M., Verberne, M.E., DeRuiter, M.C., Poelmann, R.E. and Gittenberger-de Groot, A.C. (1998) Neural crest cell contribution to the developing circulatory system: implications for vascular morphology? *Circ. Res.*, **82**, 221–231.
38. Tamisier, D., Goutiere, F., Sidi, D., Vaksmann, G., Bruneval, P., Vouhe, P. and Leca, F. (1997) Abdominal aortic aneurysm in a child with tuberous sclerosis. *Ann. Vasc. Surg.*, **11**, 637–639.
39. Bavdekar, S.B., Vaideeswar, P., Bakune, R.H., Sahu, D.K. and Kamat, J.R. (2000) Aortic aneurysm in a child with tuberous sclerosis. *Indian Pediatr.*, **37**, 319–322.
40. Jost, C.J., Głowiczki, P., Edwards, W.D., Stanson, A.W., Joyce, J.W. and Pairolero, P.C. (2001) Aortic aneurysms in children and young adults with tuberous sclerosis: report of two cases and review of the literature. *J. Vasc. Surg.*, **33**, 639–642.
41. Rosser, T.L., Vezina, G. and Packer, R.J. (2005) Cerebrovascular abnormalities in a population of children with neurofibromatosis type 1. *Neurology*, **64**, 553–555.
42. Friedman, J.M., Arbiser, J., Epstein, J.A., Gutmann, D.H., Huot, S.J., Lin, A.E., McManus, B. and Korf, B.R. (2002) Cardiovascular disease in neurofibromatosis 1: report of the NF1 Cardiovascular Task Force. *Genet. Med.*, **4**, 105–111.
43. Hamilton, S.J. and Friedman, J.M. (2000) Insights into the pathogenesis of neurofibromatosis 1 vasculopathy. *Clin. Genet.*, **58**, 341–344.
44. Stewart, D.R., Cogan, J.D., Kramer, M.R., Miller, W.T. Jr, Christiansen, L.E., Pauciulo, M.W., Messiaen, L.M., Tu, G.S., Thompson, W.H., Pyeritz, R.E. *et al.* (2007) Is pulmonary arterial hypertension in neurofibromatosis type 1 secondary to a plexogenic arteriopathy? *Chest*, **132**, 798–808.
45. Dasgupta, B. and Gutmann, D.H. (2003) Neurofibromatosis 1: closing the GAP between mice and men. *Curr. Opin. Genet. Dev.*, **13**, 20–27.
46. Xu, J., Ismat, F.A., Wang, T., Yang, J. and Epstein, J.A. (2007) NF1 regulates a Ras-dependent vascular smooth muscle proliferative injury response. *Circulation*, **116**, 2148–2156.
47. Lasater, E.A., Bessler, W.K., Mead, L.E., Horn, W.E., Clapp, D.W., Conway, S.J., Ingram, D.A. and Li, F. (2008) Nf1^{+/-} mice have increased neointima formation via hyperactivation of a Gleevec sensitive molecular pathway. *Hum. Mol. Genet.*, **17**, 2336–2344.
48. Li, F., Munchhof, A.M., White, H.A., Mead, L.E., Krier, T.R., Fenoglio, A., Chen, S., Wu, X., Cai, S., Yang, F.C. and Ingram, D.A. (2006) Neurofibromin is a novel regulator of RAS-induced signals in primary vascular smooth muscle cells. *Hum. Mol. Genet.*, **15**, 1921–1930.
49. Milewicz, D.M., Guo, D., Tran-Fadulu, V., Lafont, A., Papke, C., Inamoto, S. and Pannu, H. (2008) Genetic basis of thoracic aortic aneurysms and dissections: focus on smooth muscle cell contractile dysfunction. *Annu. Rev. Genomics Hum. Genet.*, **9**, 283–302.
50. Ikonomidis, J.S., Gibson, W.C., Gardner, J., Sweterlitsch, S., Thompson, R.P., Mukherjee, R. and Spinale, F.G. (2003) A murine model of thoracic aortic aneurysms. *J. Surg. Res.*, **115**, 157–163.